Received: 23 June 2024 | Revised: 14 August 2024 | Accepted: 5 December 2024 | Published online: 12 December 2024

RESEARCH ARTICLE

Journal of Optics and Photonics Research
2024, Vol. 00(00) 1–8
DOI: 10.47852/bonviewJOPR42023675

BON VIEW PUBLISHING

Mode-Group (De)Multiplexer Based on Directional Coupler Formed by Heterogeneous Integrated Waveguides

Jiali Zhang[1,2,3,4], Kedi Peng[1,2,3,4], Jiaqi Ran[1,2,3,4], Yaomin Wu[1,2], Jiadong Xiao[1,2], Yujian Chen[1,2], Yarou Chen[1,2], Ou Xu[1,2,3,4,*] and Quandong Huang[1,2,3,4,*]

[1]*Institute of Advanced Photonics Technology, Guangdong University of Technology, China*

[2]*School of Information Engineering, Guangdong University of Technology, China*

[3]*Key Laboratory of Photonic Technology for Integrated Sensing and Communication, Ministry of Education of China, Guangdong University of Technology, China*

[4]*Guangdong Provincial Key Laboratory of Information Photonics Technology, Guangdong University of Technology, China*

Abstract: A simple mode-group (de)multiplexer utilizing a co-planar directional coupler formed by heterogeneous waveguides is proposed, which features two few-mode cores with different refractive indices and heights. The proposed device enables the control of mode-group (de) multiplexing between two few-mode cores, i.e., for manipulating both the E_{21} and E_{12} modes as a mode group. A three-mode (de)multiplexer is designed and fabricated with polymer materials through multi-step photolithography to demonstrate the proposed methodology, where only the high-order modes couple between two few-mode cores. For E_{21} mode and E_{12} mode, a coupling ratio higher than 90.6% and 89.9% is measured of our device within the C-band, ranging from 1530 to 1565 nm. A low polarization state sensitivity is confirmed by modal crosstalk lower than −9.8 dB and −9.5 dB to the E_{11} mode from E_{21} mode and E_{12} mode, respectively. A modal crosstalk lower than −17.8 dB to both the E_{21} and E_{12} modes from E_{11} mode is represented. The proposed mode-group (de)multiplexer can be further developed to manipulate more guide mode groups, and the crosstalks can be further decreased by introducing horizontal and vertical tapers during the fabrication. The device proposed can find application in photonic integrated chips where mode-group manipulations are required.

Keywords: mode multiplexer, optical waveguide device, lithography, directional coupler, polymer waveguide

1. Introduction

The continuously growing data volume presents a new demand for optical communication systems with the development of new applications, such as big data, cloud, and Internet of Things; optical communications data traffic has experienced explosive growth in recent years [1, 2]. To keep up with the pace of data transmission growth, various technologies have been investigated to cope with the exponential increase in data traffic, with multiplexing technology representing a viable option for increasing the fiber transmission capacity through parallelism of physical dimensions in frequency, polarization, time, quadrature, and space [3]. Space division multiplexing technology, as an available technique for enhancing the transmission capacity and spectral efficiency in optical communication [4], can be implemented through various schemes: multicore multiplexing [5], mode division multiplexing (MDM) [6], and their combinations. MDM technology allows for multiple spatial pathways available in few-mode fibers to significantly enhance transmission capacity through parallelism of spatial modes, making it one of the promising efficient methods. Recently, an optical communication system using MDM and wavelength division multiplexing has been demonstrated in the mid-infrared region, which multiplexes three wavelengths of ~3.4 μm, two OAM modes, and transmits 50-Gbit/s QPSK signals. Compared to previous mid-IR transmission with single beam and channel, the proposed system achieves a ~30x improvement in transmission capacity [7].

Mode (de)multiplexer, which allows for combining and separating of different modes in an optical communication system, is a crucial component of MDM system. Currently, many photonic integrated devices, including Y-junctions, photonic lanterns, multimode interferometers, and directional couplers (DCs) [8–13], are explored to implement mode (de)multiplexing.

*Corresponding authors: Ou Xu, Institute of Advanced Photonics Technology, School of Information Engineering, Key Laboratory of Photonic Technology for Integrated Sensing and Communication, Ministry of Education of China, and Guangdong Provincial Key Laboratory of Information Photonics Technology, Guangdong University of Technology, China. Email: xuou@gdut.edu.cn and Quandong Huang, Institute of Advanced Photonics Technology, School of Information Engineering, Key Laboratory of Photonic Technology for Integrated Sensing and Communication, Ministry of Education of China, and Guangdong Provincial Key Laboratory of Information Photonics Technology, Guangdong University of Technology, China. Email: qdhuang@gdut.edu.cn

Among these reported devices, DCs attract more attention due to their merits of flexibility and scalability in the design. Theory of parallel waveguide coupling was proposed and analyzed by S. Miller in 1954 [14], and many horizontal DCs were developed later. For the mode manipulating devices, a three-mode (de) multiplexer using parallel waveguides with a uniform height has been demonstrated [15]. However, parallel waveguides cannot establish coupling between modes with horizontally symmetric modes as exemplified by the LP_{01} mode and LP_{11b} mode, and a mode rotator which breaks the vertical symmetric by modifying the mode overlap integral is used to figure out this problem. With a mode rotator by using a trench in the straight few-mode waveguide [16], a PLC-based mode (de)multiplexer for four modes has been demonstrated [17]. Another way to break the symmetry is to introduce waveguide formed by three-dimensional (3D) structures, such as vertical DCs or horizontal DCs with non-uniform heights [18, 19]. However, silicon platform-based devices make the fabrication of 3D waveguides difficult, and some challenges exist in the fabrication due to the characteristics of silicon materials [20].

Polymer material, based on photolithography technology, allows the formation of multilayer and 3D waveguide structures in an easy way, which provides a particularly flexible methodology for developing devices that manipulate all modes regardless of the mode symmetric whether they are in the horizontal or vertical directions. Recently, adiabatic-tapered waveguides employed in DCs have emerged as a viable solution for achieving broadband mode (de)multiplexing [21, 22]. To manipulate more modes with a simpler design, the efficient multiplexing of three modes with integrating horizontal and vertical DCs forming 3D waveguide has been demonstrated [23]. However, in the case of all reported DC-based mode (de) multiplexers, the waveguide cores have an identical refractive index. The above design means that few-mode cores (FMCs) need to couple different high-order modes to single-mode cores (SMCs) and vice versa, which control only one mode with one SMC core. As the number of the (de)multiplexed mode numbers increases, more DCs are required, making design and fabrication more difficult.

In this paper, we present a co-planar DC composed of two FMCs, where one of the FMCs possesses a higher refractive index than the other one. We can manipulate the mode groups regardless of their symmetry in the same DC with lower crosstalk in such a heterogeneous waveguide design, rather than an optical component that manipulates only one guide mode. In the experimental demonstration, a mode-group (de)multiplexer for manipulating three modes is designed and fabricated with polymer materials via multi-step photolithography. For the E_{21} and E_{12} modes, the fabricated chips demonstrate a coupling ratio higher than 90.6% and 89.9% in the C-band, and the measured modal crosstalks to E_{11} modes are lower than −9.5 dB, demonstrating the state of polarization is insensitivity. For the E_{11} mode, modal crosstalk lower than −17.8 dB to E_{21} and E_{12} modes is measured. The crosstalk can be further reduced by a tapered waveguide [23, 24] or 2D material-embedded waveguide [25]. The device can be further applied in photonic integrated chips where mode group manipulating is required as well as increasing the integration of chips.

2. Design and Methodology

The structure of the mode-group (de)multiplexer is shown in Figure 1, which is composed of two FMCs with different widths, heights, and refractive indices, where each FMC supports E_{11}, E_{21}, and E_{12} modes as guided mode. In the design, the FMC 2 possesses a higher refractive index than FMC 1, making the difference in effective refractive index of the E_{11} mode between

Figure 1
The structure of the mode-group (de)multiplexer comprises two few-mode hybrid cores with different dimensions and materials

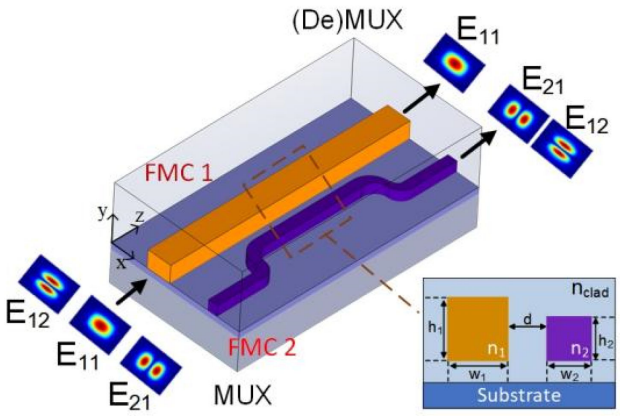

the two cores significant. As a result, it is possible to avoid the significant coupling of the fundamental modes between the two FMCs. Conversely, strong coupling of both the E_{21} modes and the E_{12} modes can be achieved simultaneously between the two FMCs by controlling the parameters of the two FMCs, including heights, widths, and the refractive index.

As shown in Figure 2 for the guide modes, the strong coupling between modes occurs between two FMCs when the guide modes meet the phase-matching condition, which relies on the match of effective refractive indices. For guided modes, the dimension of the FMCs determines the effective refractive index in the waveguide design theory. Thanks to the hybrid-core design, we can realize the strong coupling of the E_{21} and E_{12} modes while having a small effect on the E_{11} mode between the two FMCs.

We determine the effective indices of the three guide modes in two FMCs by using a mode solver commercial software based on the full-vector finite-element method (COMSOL). The refractive indices of FMC 1, FMC 2, and the cladding are set at 1.564, 1.569, and 1.559, respectively. These parameters are also the same as those used in the fabrication. We design the core heights of FMC 1 and FMC 2 to be $h_1 = 10$ μm and $h_2 = 6.5$ μm, respectively. Then we calculate the dispersion of guide modes against the core widths. The simulation results of the guide modes against the core widths

Figure 2
The phase-matching condition for the E_{21} mode and E_{12} mode between FMC 1 and FMC 2, where the effective refractive index of the E_{21} and E_{12} modes in FMC 1 is phase-matched that in FMC 2

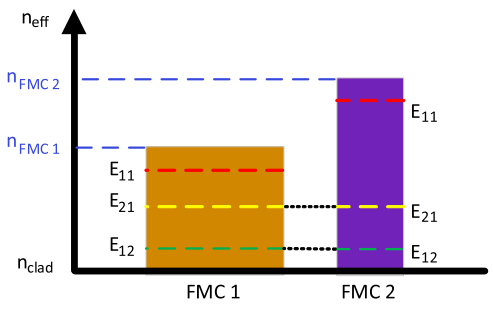

Figure 3

(a) The effective refractive indices of different TE-polarized guide modes change with the core width of FMC 1 (orange color) and the core width of FMC 2 (purple color) at 1550 nm, where the chosen widths for FMC 1 and FMC 2 are fixed at $w_1 = 11.7\,\mu$m and $w_2 = 7.2\,\mu$m for phase-matched that is highlighted by thin vertical lines. (b) The top view of the waveguide structure built in Rsoft CAD and the propagation paths with (c) the E_{11}, (d) the E_{21}, and (e) the E_{12} modes launched into FMC 1

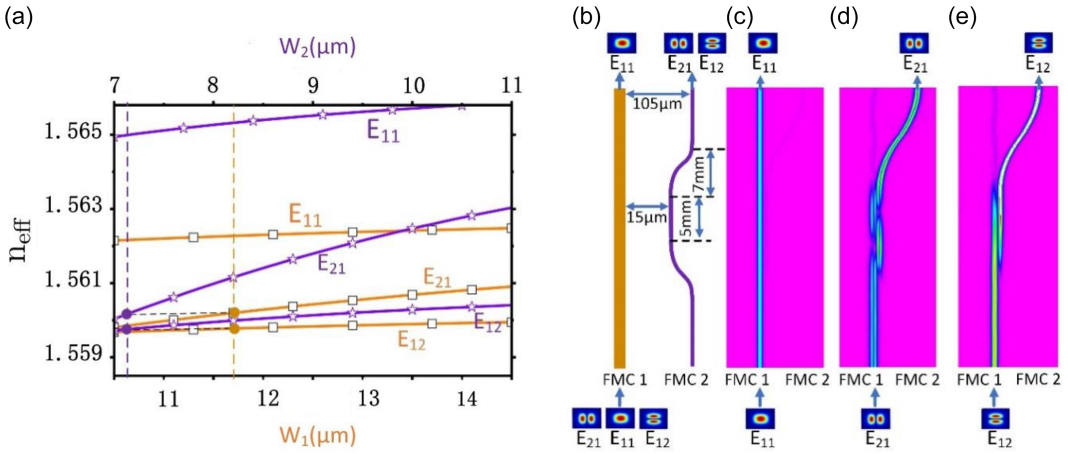

are plotted for TE polarization at the wavelength of 1550 nm, which is shown in Figure 3(a). The effective indices difference of the E_{11} mode between two FMCs is larger than 2×10^{-3}, which indicates that significant coupling is unlikely to happen for the E_{11} mode between the two FMCs regardless of the changes in their core sizes.

To achieve the phase-matched of both the E_{21} and E_{12} modes, we choose core widths to be $w_1 = 11.7$ μm and $w_2 = 7.2$ μm that allow E_{21} mode and E_{12} mode couple between the two core regions effectively. To confirm the length of DC, we use commercial software (Rsoft) with 3D finite-difference beam propagation method to study the mode coupling for the analysis. Figure 3(b) illustrates the top view of the waveguide constructed in Rsoft. The mode propagation field of each guided mode is respectively illustrated in Figure 3(c), (d), and (e). The gap between two parallel waveguides is designed to be 15 μm to ensure the best experimental conditions, and the length for the parallel waveguides is designed to be 5 mm with two symmetric S-bend lengths is calculated to be 7 mm which is based on the gap, and the outlet of two FMCs with a separation of 105 μm both in the input and output thanks to the S-bend. The design determines the coupling length and gives the horizontal space for the coupling between the waveguide and fiber. As shown in Figure 3(c), (d), and (e), the E_{11} mode stays at Core 1, where the coupling ratio is almost equal to zero. Moreover, the E_{21} and E_{12} modes are coupled to Core 2 with most of the optical power and then output from Core 2 as expected. As a result, such a device can function as an effective fundamental-mode-pass mode-group mode (de)multiplexer.

The performances of the mode-group (de)multiplexing can be characterized in the form of coupling ratios for the E_{mn} (where $mn = 11$, 21, and 12) modes from FMC 1 to FMC 2, which are formulated as follows:

$$CR_{mn} = \frac{P_{out-mn}}{P_{out-total}} \tag{1}$$

where P_{out-mn} is the output power of E_{mn} mode in FMC 2 when launching the E_{mn} mode into FMC 1, and $P_{out-total}$ is the overall power output from two FMCs. For the E_{11}, E_{21}, and E_{12} modes, the simulated coupling ratios are respectively labeled as CR_{11}, CR_{21}, and CR_{12} as shown in Figure 4. For TE and TM polarization, the CR_{21} is respectively greater than 95.0% and 96.2% in the C-band, and the CR_{12} is respectively greater than 90.0% and 91.2% in the C-band, whereas the CR_{11} is respectively lower than 0.02% and 0.01%.

Figure 4

Calculated coupling ratios for (a) TE and (b) TM polarizations of different guided modes

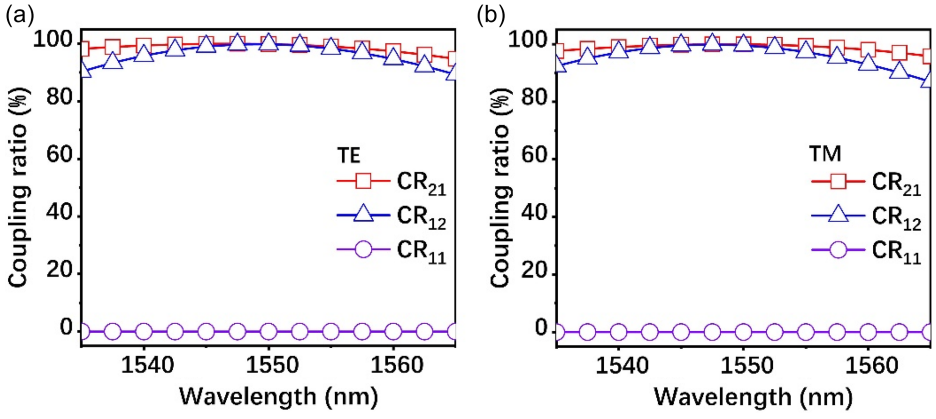

Figure 5
The crosstalk of the residual power with launching the E_{21} and E_{12} modes into the FMC 1 and the weak coupling of the E_{11} mode from FMC 1 to FMC 2 for (a) the TE, (b) the TM polarizations

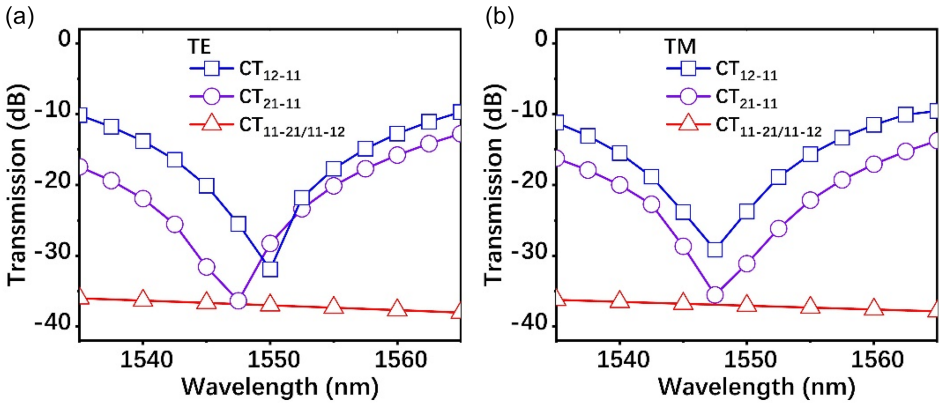

Weak couplings from the unexpected modes occur when the intended modes are launched into FMC 1, which may lead to the modal crosstalk between different spatial modes. Also, the residual powers of the intended modes are classified as crosstalks. As a result, the modal crosstalk can be determined by launching the intended mode at the MUX port of FMC 1, and then the output power of all cores except the expected core is crosstalk, which can be defined as follows:

$$CT_{mn-pq} = 10log_{10}\frac{P_{out-pq}}{P_{out-mn}}(pq \neq mn) \quad (2)$$

For TE and TM polarizations, the simulated crosstalk of the $CT_{11\text{-}21/11\text{-}12}$, $CT_{21\text{-}11}$, and $CT_{12\text{-}11}$ is shown in Figure 5(a) and (b), respectively. By using Equation (2), The $CT_{11\text{-}21/11\text{-}12}$, $CT_{21\text{-}11}$, and $CT_{12\text{-}11}$ are lower than − 9.7 dB and − 9.6 dB at C-band for TE and TM polarizations. Then we calculate the device tolerance with different widths of the FMCs. As shown in Figure 6, the FMC 1 and FMC 2 width variation with coupling ratios larger than 90% range from 11.58 (11.60) μm to 12.15 (12.17) μm and 7.17 (7.16) μm to 7.33 (7.32) μm for the TE(TM) polarization, respectively.

3. Fabrication and Characterization

The mode-group (de)multiplexer is fabricated using EpoCore and EpoClad polymer materials (Micro resist technology, GmbH) as core and cladding materials, respectively, following design parameters via an in-house fabrication facility, where the fabrication steps are shown in Figure 7. For the supporting substrate, a silicon substrate with an orientation of <100> is selected and activated by plasma cleaning. The lower cladding is formed by spin-coating the EpoClad polymer onto the silicon substrate. After the EpoCore polymer material with a higher refractive index is spin-coated onto the lower cladding, then the pattern of the FMC 2 is formed by using photolithography on the same plane of the lower cladding. Later, the FMC 2 is cured before the spin-coating of EpoCore polymer material with a lower refractive index, so the FMC 1 is then formed on the same plane of the lower cladding by using photolithography and the FMC 2 does not affect the fabrication of the FMC 1. Conversely, the construction of FMC 1 as the first step will impact the fabrication process of FMC 2 because of its large size. Finally, the upper cladding is formed by spin-coating the EpoClad polymer on the

Figure 6
Coupling ratios of the E_{21} mode and the E_{12} mode with the variation of (a) the FMC 1 width and (b) the FMC 2 width

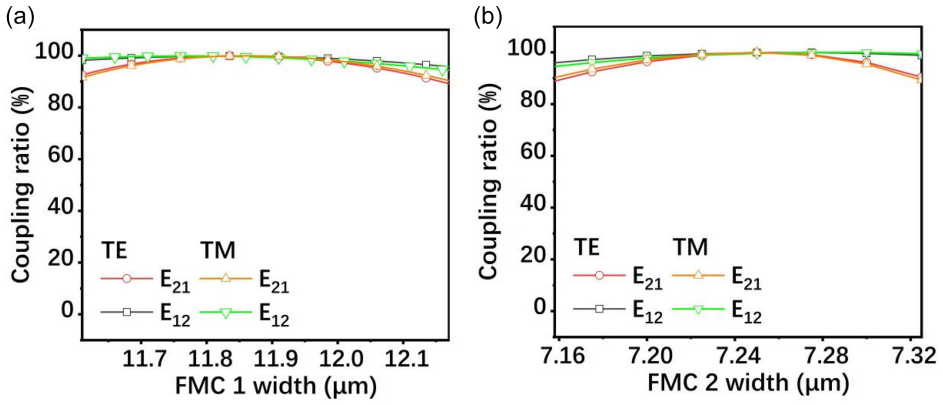

Figure 7
Fabrication steps of the proposed mode-group (de) multiplexer

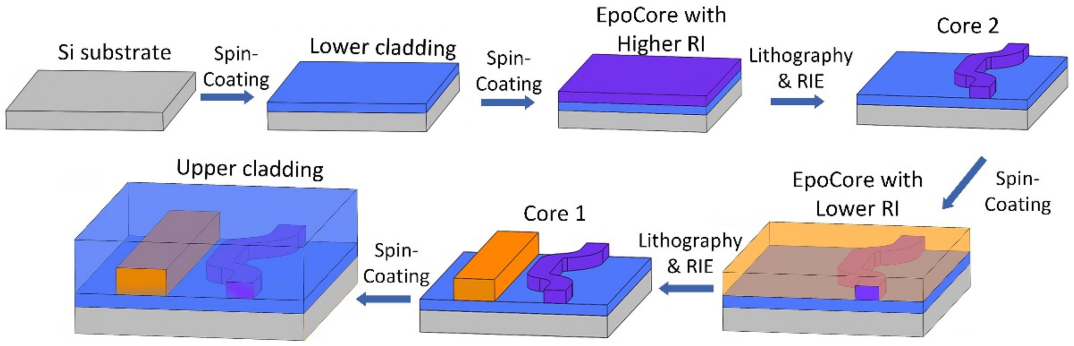

Figure 8
Device top view during the fabrication of (a) the coupling region and (b) the outlet region; (c) the end face

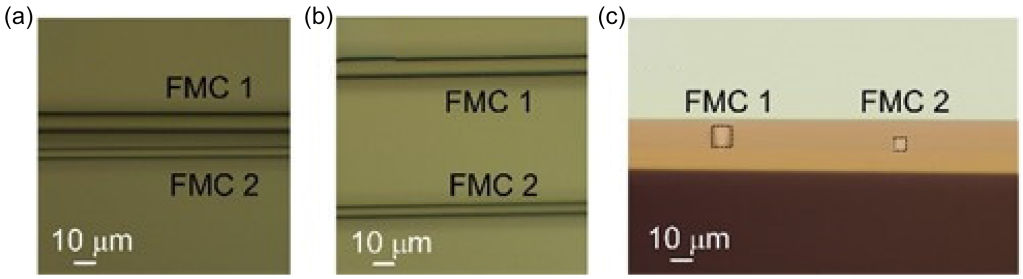

top of the device. At last, we can achieve two FMCs DC formed by heterogeneous waveguides via this fabrication technology [26].

Top views and end face of the photonic circuits during the fabrication are shown in Figure 8. The coupling region of the chip is shown in Figure 8(a), where FMC 2 possesses a higher refractive index than FMC 1. FMC 1 and FMC 2 are of different heights. The outlet of the photonic circuits is shown in Figure 8(b), where the interval of the FMC 1 and FMC 2 is about 105 μm. Figure 8(c) shows the end face of the fabricated circuits, where the end face confirms that the FMC 1 and FMC 2 are fabricated with different heights and materials. By using the multi-step photolithography methodology, we can realize the fabrication of 3D waveguide structures with different materials and core dimensions (both the core width and height). The proposed methodology can further simplify the fabrication process such as introducing a middle cladding or additional RIE trimming with metal mask [18, 23].

The fabricated mode multiplex is measured by experimental measurement setup as shown in Figure 9. A tunable light source is applied to generate the light in the C-band. A fiber mode converter is selected to generate the high-order modes (such as the E_{21} and E_{12} modes) as the input high-order mode source [27]. The

Figure 9
Experimental setups for the device measurement

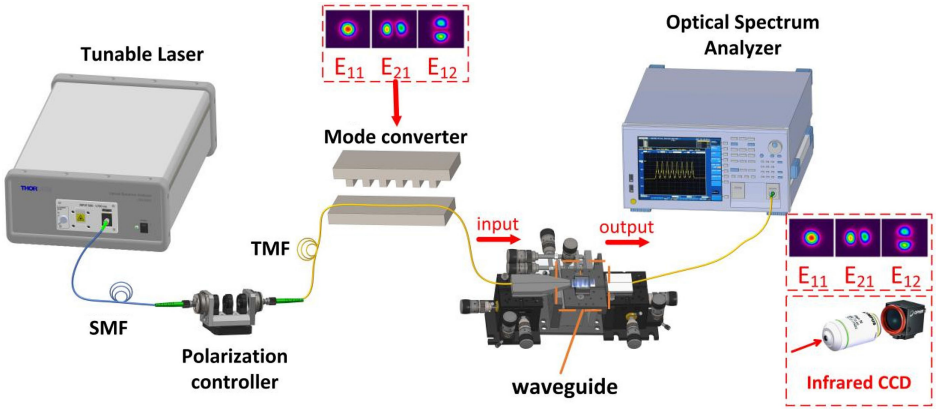

Figure 10
(a) Fabricated chip and (b) the captured near-field patterns for the E_{11}, E_{21}, and E_{12} modes from the FMC 1 and FMC 2

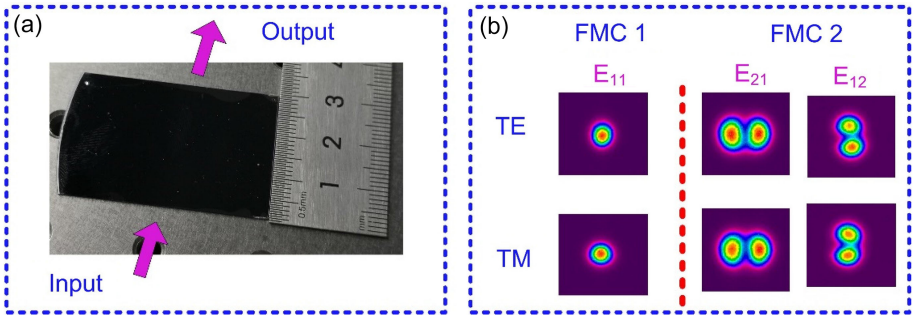

Figure 11
Coupling ratios of the mode-group (de)multiplexer for (a) the TE and (b) the TM polarizations of the E_{21} and E_{12} modes

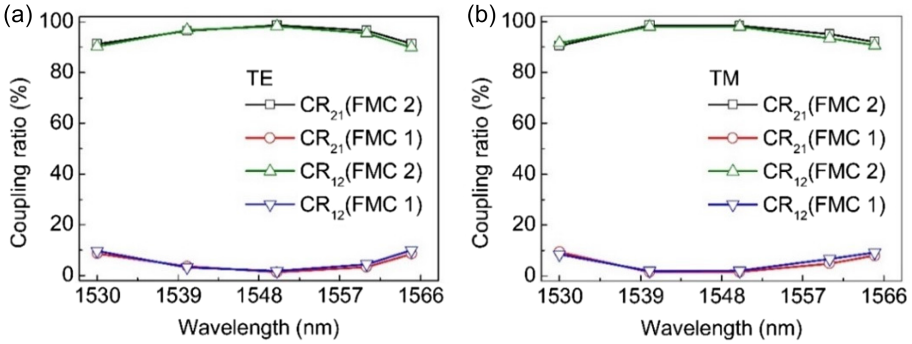

fabricated mode-group (de)multiplexer on a chip is shown in Figure 10(a), where the length of the chip including the input and output ports is about 2.9 cm. The intended mode can be launched into the chip from either end or any port of the chip as desired. The mode-group multiplexer serves to couple both the E_{21} and E_{12} modes from FMC 1 to FMC 2 and vice versa, while the remaining fundamental mode stays in the FMC that was launched in and propagates along the FMC, and at last the fundamental mode outputs from the output port of the FMC where it is launched into. For example, when we launch the three modes into the FMC 1, the E_{11} mode stays in and output from the FMC 1 while the E_{21} and E_{12} modes are both coupled to FMC 2 and then output from the FMC 2. Using the infrared CCD (Ophir-Spiricon), the captured near-field patterns from the output ports of the FMC 1 and FMC 2 for TE and TM polarizations are shown in Figure 10(b). The experimental results confirm that the device can serve as a mode-group (de)multiplexer to manipulate the mode groups.

The powers for each mode output from the FMC 1 and FMC 2 of the fabricated mode multiplexer are measured by a photodetector. By using (1), the coupling ratios of the E_{21} and E_{12} modes are calculated as CR_{21} and CR_{12} for outputs from FMC 2, and similarly, CR_{21} and CR_{12} for output from FMC 1. As shown in Figure 11, the CR_{21}(output from the FMC 2) and CR_{12}(output from the FMC 2) are higher than 91.3% (90.6%) and 89.9% (90.8%), while the CR_{21}(output from the FMC 1) and CR_{12}(output from the FMC 1) are lower than 8.7% (9.4%) and 9.2%, respectively, in the C-band. The CR_{11} is lower than 0.1% (0.1%), which is not shown in Figure 11. The device is polarization-insensitive as confirmed by experimental results. The insertion loss that includes the coupling loss and propagation loss for the E_{11}, E_{21}, and E_{12} modes is measured to be about 8.2 dB, 9.1dB, and 9.5 dB, respectively. The insertion loss caused by the material that is operated at 800 nm can be greatly reduced by using low loss material at 1550 nm.

The residual powers of the E_{21} and E_{12} modes in the FMC 1 and the weak coupling of the E_{11} mode from the FMC 1 to FMC 2 are the crosstalks. By using Equation (2), the crosstalks are analyzed in the experiment as well. As shown in Figure 12, for TE and TM polarization, the crosstalks are lower than −18.2 dB and −17.8 dB

Figure 12
Crosstalks of the mode-group (de)multiplexer caused by the E_{11} mode and the residual power of the E_{21} and E_{12} modes

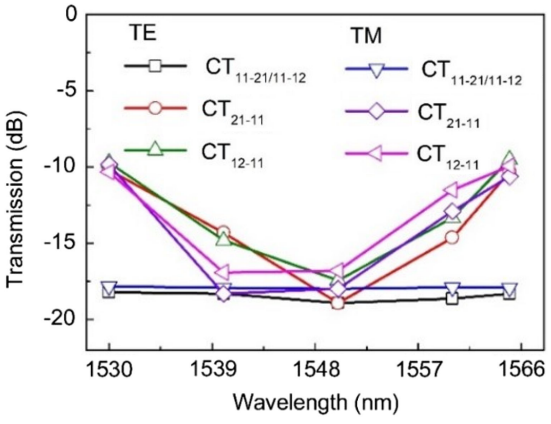

to the E_{21} and E_{12} modes from E_{11} mode ($CT_{11\text{-}21/11\text{-}12}$), respectively, and the crosstalks are lower than −10.2 dB and −9.8 dB to the E_{11} mode from E_{21} mode, and −9.5 dB and −9.9 dB to the E_{11} mode from E_{12} mode, respectively. The crosstalks caused by the E_{21} and E_{12} modes to the E_{11} mode can be further decreased by introducing horizontal and vertical tapers during the fabrication [23].

4. Conclusion

Current DC-based mode multiplexers require coupling higher-order modes in FMCs to the fundamental mode in SMCs or vice versa, which can only manipulate one mode with two DCs. To manipulate more modes with less DCs, we propose a mode-group (de)multiplexer based on co-planar DC formed by heterogeneous waveguides, which is fabricated via multi-step photolithography. The simple, scalable, and effective mode-group multiplexer opens new possibilities in designing devices for controlling modes, such as mode-dependent-loss compensators, mode filters, etc. The multi-step photolithography design methodology could realize photonic integrated chips with a simpler structure in the applications. The design methodology of multi-step photolithography could achieve the realization of photonic integrated chips with a simpler structure in the applications.

Funding Support

This work was supported by the National Natural Science Foundation of China (Grant No. 62205067), NSFC-NCN (Grant No. 62361136584), and Guangzhou Basic and Applied Basic Research Scheme (Grant No. 2023A04J1708).

Ethical Statement

This study does not contain any studies with human or animal subjects performed by any of the authors.

Conflicts of Interest

The authors declare that they have no conflicts of interest to this work.

Data Availability Statement

Data are available from the corresponding author upon reasonable request.

Author Contribution Statement

Jiali Zhang: Formal analysis, Investigation, Data curation, Writing – original draft, Writing – review & editing, Visualization. **Kedi Peng:** Software, Writing – review & editing, Visualization. **Jiaqi Ran:** Writing – review & editing. **Yaomin Wu:** Writing – review & editing. **Jiadong Xiao:** Writing – review & editing. **Yujian Chen:** Writing – review & editing. **Yarou Chen:** Writing – review & editing. **Ou Xu:** Validation, Supervision. **Quandong Huang:** Conceptualization, Methodology, Validation, Formal analysis, Investigation, Resources, Data curation, Writing – original draft, Writing – review & editing, Visualization, Supervision, Project administration, Funding acquisition.

References

[1] Richardson, D. J., Fini, J. M., & Nelson, L. E. (2013). Space-division multiplexing in optical fibres. *Nature Photonics*, *7*(5), 354–362.

[2] Mizuno, T., & Miyamoto, Y. (2017). High-capacity dense space division multiplexing transmission. *Optical Fiber Technology*, *35*, 108–117.

[3] Winzer, P. J. (2014). Spatial multiplexing in fiber optics: The 10x scaling of metro/core capacities. *Bell Labs Technical Journal*, *19*, 22–30.

[4] Puttnam, B. J., Rademacher, G., & Luís, R. S. (2021). Space-division multiplexing for optical fiber communications. *Optica*, *8*(9), 1186–1203.

[5] Chen, X., Zakharian, A. R., Johnson, S., Hurley, J. E., Butler, D. L., Bennett, K. W., . . . , & Li, M. J. (2022). Demonstration of 1 Tb/s transmission over 6.3-km 1 × 4 linear array multicore fiber with standard 125-μm cladding. *Optical Fiber Technology*, *71*, 102941.

[6] Du, J., Shen, W., Liu, J., Chen, Y., Chen, X., & He, Z. (2021). Mode division multiplexing: From photonic integration to optical fiber transmission. *Chinese Optics Letters*, *19*(9), 091301.

[7] Zou, K., Pang, K., Song, H., Fan, J., Zhao, Z., Song, H., . . . , & Willner, A. E. (2022). High-capacity free-space optical communications using wavelength-and mode-division-multiplexing in the mid-infrared region. *Nature Communications*, *13*(1), 7662.

[8] González-Andrade, D., Olivares, I., de Cabo, R. F., Vilas, J., Dias, A., & Velasco, A. V. (2023). Broadband three-mode converter and multiplexer based on cascaded symmetric Y-junctions and subwavelength engineered MMI and phase shifters. *Optics & Laser Technology*, *164*, 109513.

[9] Eznaveh, Z. S., Antonio-Lopez, J. E., Zacarias, J. A., Schülzgen, A., Okonkwo, C. M., & Correa, R. A. (2017). All-fiber few-mode multicore photonic lantern mode multiplexer. *Optics Express*, *25*(14), 16701–16707.

[10] Jiang, W., Xie, L., & Zhang, L. (2023). Design and experimental demonstration of a silicon five-mode (de) multiplexer based on multi-phase matching condition. *Optics Express*, *31*(20), 33343–33354.

[11] Su, Y., Liu, D., & Zhang, M. (2022). Sb_2Se_3-assisted reconfigurable broadband Y-junction. *Optics Express*, *30*(22), 40379–40388.

[12] Sun, S., Yu, Q., Che, Y., Lian, T., Xie, Y., Zhang, D., & Wang, X. (2024). Mode-insensitive and mode-selective optical switch based on asymmetric Y-junctions and MMI couplers. *Photonics Research*, *12*(3), 423–430.

[13] Mao, S., Cheng, L., Zhao, C., Wang, Y., Li, Q., & Fu, H. Y. (2023). Compact hybrid five-mode multiplexer based on asymmetric directional couplers with constant bus waveguide width. *Optics Letters*, *48*(10), 2607–2610.

[14] Miller, S. E. (1954). Coupled wave theory and waveguide applications. *Bell System Technical Journal*, *33*(3), 661–719.

[15] Hanzawa, N., Saitoh, K., Sakamoto, T., Matsui, T., Tsujikawa, K., Koshiba, M., & Yamamoto, F. (2014). Mode multi/demultiplexing with parallel waveguide for mode division multiplexed transmission. *Optics Express*, *22*(24), 29321–29330.

[16] Saitoh, K., Uematsu, T., Hanzawa, N., Ishizaka, Y., Masumoto, K., Sakamoto, T., . . . , & Yamamoto, F. (2014). PLC-based LP 11 mode rotator for mode-division multiplexing transmission. *Optics Express*, *22*(16), 19117–19130.

[17] Hanzawa, N., Saitoh, K., Sakamoto, T., Matsui, T., Tsujikawa, K., Uematsu, T., & Yamamoto, F. (2015). PLC-based four-mode multi/demultiplexer with LP 11 mode rotator on one chip. *Journal of Lightwave Technology*, *33*(6), 1161–1165.

[18] Zhao, W. K., Chen, K. X., Wu, J. Y., & Chiang, K. S. (2017). Horizontal directional coupler formed with waveguides of different heights for mode-division multiplexing. *IEEE Photonics Journal*, *9*(5), 1–9.

[19] Watanabe, T., & Kokubun, Y. (2015). Demonstration of mode-evolutional multiplexer for few-mode fibers using stacked polymer waveguide. *IEEE Photonics Journal*, *7*(6), 1–11.

[20] Hiraki, T., Tsuchizawa, T., Nishi, H., Yamamoto, T., & Yamada, K. (2015). Monolithically integrated mode multiplexer/de-multiplexer on three-dimensional SiOx-waveguide platform. In *Optical Fiber Communication Conference*, W1A-2.

[21] Gross, S., Riesen, N., Love, J. D., & Withford, M. J. (2014). Three-dimensional ultra-broadband integrated tapered mode multiplexers. *Laser & Photonics Reviews*, *8*(5), L81–L85.

[22] Zhao, W. K., Chen, K. X., & Wu, J. Y. (2019). Broadband mode multiplexer formed with non-planar tapered directional couplers. *IEEE Photonics Technology Letters*, *31*(2), 169–172.

[23] Huang, Q., He, J., Zheng, Z., & Zhou, X. (2024). Ultra-broadband and low-modal-crosstalk mode multiplexer based on cascaded vertical directional couplers formed by adiabatic-tapered waveguides without mode conversion. *Journal of Lightwave Technology*, *42*(5), 1566–1572.

[24] Sun, L., & Zhang, R. (2021). Metamaterial-based ultrashort multimode waveguide taper with low intermodal crosstalk. *Optics Express*, *29*(5), 7124–7133.

[25] Jiang, L., Jiang, W., & Chiang, K. S. (2023). All-optical tunable filter with a graphene-buried long-period waveguide grating. *IEEE Photonics Journal*, *15*(4), 1–6.

[26] Huang, Q., Ran, J., Peng, K., He, J., Chen, Q., & Zhou, X. (2024). Hybrid-core co-planar waveguide mode multiplexer fabricated by multi-step photolithography for high-order-mode-passed guide mode manipulating. *Optics & Laser Technology*, *175*, 110798.

[27] Zhong, L., Huang, Q., Zhang, J., Zheng, Z., Li, J., & Xu, O. (2023). Reconfigurable ultra-broadband mode converter based on a two-mode fiber with pressure-loaded phase-shifted long-period alloyed waveguide grating. *Optics Express*, *31*(5), 8286–8295.

How to Cite: Zhang, J., Peng, K., Ran, J., Wu, Y., Xiao, J., Chen, Y., . . . , & Huang, Q. (2024). Mode-Group (De)Multiplexer Based on Directional Coupler Formed by Heterogeneous Integrated Waveguides. *Journal of Optics and Photonics Research*. https://doi.org/10.47852/bonviewJOPR42023675